Conf-910869--24

GA–A20697

ICRF HEATING EXPERIMENTS ON DIII–D

by
R.I. PINSKER, M.J. MAYBERRY, C.C. PETTY, M. PORKOLAB,
S.C. CHIU, R. PRATER, F.W. BAITY, R.H. GOULDING,
and D.J. HOFFMAN

OCTOBER 1991

GENERAL ATOMICS

GA-A--20697

DE92 002948

GA-A20697

ICRF HEATING EXPERIMENTS ON DIII–D

by
R.I. PINSKER, M.J. MAYBERRY, C.C. PETTY, M. PORKOLAB,*
S.C. CHIU, R. PRATER, F.W. BAITY,† R.H. GOULDING,†
and D.J. HOFFMAN†

This is a preprint of a paper presented at the Ninth Topical Conference on the Radio Frequency, August 19–21, 1991, in Charleston, South Carolina, and to be printed in the *Proceedings*.

Work supported by
U.S. Department of Energy
Contract Nos. DE-AC03-89ER51114 and DE-AC05-84OR21400

* Plasma Fusion Center, MIT, USA.
† Oak Ridge National Laboratory, USA.

GENERAL ATOMICS PROJECT 3466
OCTOBER 1991

GENERAL ATOMICS

ICRF HEATING EXPERIMENTS ON DIII–D*

R.I. Pinsker, M.J. Mayberry, C.C. Petty, M. Porkolab,†
S.C. Chiu, R. Prater
General Atomics, P.O. Box 85608, San Diego, California 92138-5608
F.W. Baity, R.H. Goulding, D.J. Hoffman
Oak Ridge National Laboratory, Oak Ridge, Tennessee 37831

ABSTRACT

Fast wave ICRH in the fundamental hydrogen minority and second harmonic hydrogen majority regimes efficiently heats the DIII–D tokamak plasma. Agreement with confinement scaling laws derived from NBI shows that the antenna coupled efficiently to the FW and that the power was almost completely absorbed near the center of the plasma. However, when a similar antenna was oriented to excite the IBW, no efficient central heating regime was found. These experiments covered a very wide range of experimental conditions and configurations. The results show that either the antenna did not couple efficiently to the IBW, or that the IBW did not propagate to the center of the discharge. Nonlinear effects were observed in the experiment which led to a plausible explanation of the experimental results based on nonlinear wave coupling, wave propagation, and dissipation mechanisms. Both the observed antenna coupling properties and the observed heating in the scrapeoff layer were accounted for in this scenario. These nonlinear effects limit the applicability of the conventional linear picture of IBW antenna coupling and propagation in high power, low frequency ($f \lesssim 100$ MHz) experiments.

INTRODUCTION

Experiments utilizing rf power in the 32–60 MHz range to heat the DIII–D tokamak plasma are reviewed. In one set of experiments, a two-element array of loop antennas oriented in the toroidal direction was used to launch ion Bernstein waves (IBW) either directly or by mode transformation from the electron plasma wave (EPW).[1] No evidence of efficient ion heating in the central region of the plasma was found, despite an exhaustive exploration of IBW heating regimes in both limiter and divertor discharges. A strong interaction between the edge plasma and the injected rf power was observed, including perpendicular ion heating of the edge plasma correlated with parametric decay of the pump wave fields. Detailed analysis of antenna loading data has yielded evidence of ponderomotive modification of the density profile in front of the antenna. These nonlinear phenomena limit the applicability of the linear picture of IBW antenna coupling for low frequency, high rf power density IBW heating experiments. More recent experiments, to be discussed first, have employed a four-element toroidal array of poloidally-oriented loop antennas, designed for fast wave current drive (FWCD) experiments.[2] Fast wave heating experiments have been performed at 32 and 60 MHz in the fundamental hydrogen minority, second harmonic hydrogen majority, and direct electron heating regimes.[3,4] These studies were performed as a checkout of the apparatus prior to commencing FWCD experiments, and also to provide a comparison with the previously obtained IBW data. Central rf power deposition and efficient heating of the plasma were observed. Good agreement was found between the observed global heating efficiency and that predicted by scaling laws derived from neutral beam heating data.

FAST WAVE HEATING

Efficient plasma heating was observed during FW injection at 32 MHz, as shown in Fig. 1 for a SND discharge. The central toroidal magnetic field was 2.14 T, so that the hydrogen cyclotron resonance layer passed through the center of the discharge. The hydrogen fraction in

---

* Work supported by the U.S. Department of Energy under Contract Nos. DE-AC03-89ER51114 and DE-AC05-84OR21400.

† Plasma Fusion Center, MIT, Cambridge, Massachusetts 02139

the deuterium plasma was H/(H+D) $\simeq$ 2%, as measured spectroscopically. The coupled rf power (corrected for antenna losses) was 0.92 MW. A 47 kV deuterium neutral beam at 0.93 MW was injected subsequent to the rf pulse for comparison. Both methods of heating produce a loop voltage drop, indicating electron heating. However, the central electron temperature (measured from ECE) exhibits a larger increase during the FW pulse than during NBI. The increase in total stored energy, measured from the magnetics and from the diamagnetic loop, was nearly the same for the two forms of heating. Therefore, FW heating produces a more peaked electron temperature profile than the 47 kV NBI. This is verified by direct measurement of the T_e profiles.[3] The two forms of heating also produced comparable bulk ion heating. The difference between the diamagnetic loop and magnetic measurements of the stored energy during NBI is a consequence of the substantial fast ion contribution to the stored energy in that case; the fact that the difference is negligible during FW injection indicates that the hydrogen minority tail does not represent a large fraction of the total stored energy at this rf power level.

The ratio η between the observed incremental confinement time during FW injection to the predicted incremental confinement time (using ITER-89 linear offset scaling) is a measure of the absorption efficiency. Figure 2 shows η for 19 shots in the D(H) regime under different conditions and at differing power levels; the average value is $\eta = 0.85 \pm 0.18$, confirming good absorption. This technique may be used to deduce the absorption efficiency for other heating scenarios in which good absorption is not assured or efficient antenna-wave coupling is not certain.

Applying this analysis method to a second harmonic hydrogen heating case (60 MHz, 2.1 T, H/(H+D) $\approx$ 0.53), an absorption efficiency of $\eta \simeq 0.6$ is obtained (see Fig. 3a). For this discharge the coupled FW power was 0.61 MW and the increase in plasma stored energy was 21 kJ. In the $2\Omega_H$ regime, relatively weak electron heating is observed; most of the increase in stored energy stems from ion heating. This discharge was chosen as a good comparison to a typical IBW shot at a similar power level — theoretically, IBW injection should result primarily in bulk ion heating and little or no electron heating.

ION BERNSTEIN WAVE HEATING

Ion Bernstein wave heating experiments on DIII–D covered a wide range of parameter space. High power data ($P_{rf} > 0.5$ MW) were obtained at frequencies of 32, 34, 36, 38, and 60 MHz at toroidal magnetic fields from 1.0 to 2.1 T, so that resonances ranging from $\omega = \Omega_H(2\Omega_D)$ up to $3\Omega_H(6\Omega_D)$ passed through the plasma center, in various mixtures of hydrogen, deuterium, and helium. An absorption efficiency analysis for a 38 MHz IBW discharge in the $3/2\Omega_H(3\Omega_{He^4})$ regime (previously discussed in Ref. 1) is shown in Fig. 3b. In this case, the loop voltage and hence the ohmic power increased during the rf pulse, so that while the coupled IBW power is 0.50 MW, the total change in input power is 0.83 MW. The stored energy decreased slightly during the rf pulse, and recovered immediately after the rf is switched off. This implies a negative absorption efficiency. Such a result can be explained by the fact that the radiated power increased by 0.56 MW, in excess of the increase in ohmic power, resulting in a net loss in electron heating. Since there was no ion heating from IBW to compensate for the loss in electron heating, this resulted in a net decrease in the plasma stored energy.

However, even upon reducing the radiated power loss to an acceptable level with wall conditioning (carbonization), no central heating was observed. Prior to the application of carbonization, the radiated power loss was shown to be dominated by nickel; this finding is significant since the IBW antenna has no exposed Ni-bearing surfaces while the vacuum vessel walls and protective tiles near the antenna are composed of Inconel. After carbonization, Ni levels were reduced by more than two orders of magnitude from the levels observed before carbonization in an otherwise identical shot. In addition, the increment in P_{rad} decreased from approximately $2/3P_{rf}$ to $1/3P_{rf}$ after carbonization. Under freshly carbonized wall conditions, a record for power coupled with an IBW antenna was achieved: $P_{net} > 1.0$ MW for 0.1 sec, with no deleterious effect on the discharge. However, the absorption efficiency η was still unobservably small, though at least non-negative.

These results motivated an experimental and theoretical reexamination of the fundamentals of antenna/IBW coupling. The density near the antenna determines the mechanism of coupling to the IBW. If $\omega \ll \omega_{LH} \simeq \omega_{pi}$ then the antenna should excite the IBW directly when a low order ion resonance is just behind the antenna strap.[5] In the opposite, low-edge-density limit $\omega \gg \omega_{pi}$, the antenna couples to an EPW, also referred to as the lower hybrid wave, which in turn smoothly connects to the IBW near $\omega \simeq \omega_{pi}$ (mode transformation[6]). In the DIII–D experiments, midplane Langmuir probe measurements, at the same major radius as the antenna but approximately 2 m away toroidally, indicated that the edge electron density ranged from less than $3 \times 10^9\,\mathrm{cm}^{-3}$ (approximately the minimum density measurable with the probe) to values greater than $1 \times 10^{12}\,\mathrm{cm}^{-3}$. At the frequencies used, this density range encompassed both the mode transformation (EPW coupling) and direct launch (IBW coupling) regimes. The lower edge densities were obtained in diverted discharges with a separatrix/antenna gap greater than a few centimeters, while the highest densities were measured when the plasma was either inside-wall limited or outside-limited. Diverted discharges with a small separatrix/antenna gap had edge densities such that $\omega \sim \omega_{pi}$.

The characteristics of antenna coupling in the direct IBW launch regime, where $\omega < \omega_{\mathrm{LH}}$ evaluated at the antenna, can be anticipated from the nature of the IBW dispersion, which goes from a cutoff ($k_\perp = 0$) just below integral values of ω/Ω_i to very large $k_\perp$ as the next lower integral value of ω/Ω_i is approached from above. Since the impedance seen by the antenna scales as $1/k_\perp$, the antenna loading strongly peaks when a cyclotron resonance layer is located just behind the antenna strap. The properties of the loading in the low-edge-density (mode transformation) regime are quite different, and are qualitatively similar to those of lower hybrid waveguide coupling. The loading in this regime should be larger than in the direct launch case, as $k_\perp$ is much smaller for the EPW than for the IBW at the same parallel wavelength, and nearly independent of magnetic field, since the EPW dispersion relation depends only weakly on B. In particular, no loading feature is expected at integral values of ω/Ω_i.

With an antenna/separatrix gap of less than a few centimeters, the density measured at the major radius of the IBW antenna is much higher than the lower hybrid resonance density (direct IBW launch). The theory for this case is well-developed[5,7] and can be used to quantitatively predict resistive loading. However, the expected strong peaking of the loading near integral values of ω/Ω_i has never been observed in the DIII–D experiments. Furthermore, the predicted loading even at the peak value is much lower than the measured loading. This is illustrated in Fig. 4, which shows the total resistive loading as a function of ω/Ω_H from an inside-wall limited discharge ($\omega \ll \omega_{LH}$ at the antenna radius) as a function of ω/Ω_H evaluated at the antenna major radius (38 MHz, $P_{\mathrm{net}} = 0.55$ MW). The plasma was deuterium with a hydrogen minority of about 10%. Since coupling to the $4\Omega_D$ IBW should be much more difficult than to the $2\Omega_H$ IBW, the coupling should be sensitive to the hydrogen fraction. However, in another high-edge-density discharge where the ratio H/(H+D) was varied from 0.02 to 0.12 during the rf pulse by injecting hydrogen into the deuterium discharge, no change in antenna loading was observed.

These properties of the loading could be understood if the density at the antenna face were much lower than was measured by the Langmuir probe. Unfortunately, no density measurement directly adjacent to the IBW antenna Faraday shield was possible in the DIII–D experiments. If there was substantial local density depletion, then $\omega \gg \omega_{LH}$ and the antenna would excite the EPW. As discussed above, the antenna loading would then not depend strongly on ω/Ω_i or on H/(H+D), and would be relatively large.

Such a density depletion is not unexpected, as a result of the ponderomotive force. Since the IBW antenna is oriented to excite a toroidal rf electric field, the electron quiver velocity in the antenna near field, given by $v_{D\|} = (e/m_e)E_\|/\omega$, is quite large for reasonable power densities. In the weakly nonlinear limit $v_{D\|}/v_t < 1$, in which $v_t^2 \equiv 2k(T_e + T_i)/m_e$, the density depletion due to the ponderomotive force is given by[8]

$$n_e/n_{e0} \simeq \exp(-{v_{D\|}}^2/2v_t^2) \quad .$$

For typical temperatures in the scrape-off layer ($T_e \simeq T_i \sim 10$ eV), a parallel electric field adjacent to the antenna of 250 V/cm (corresponding to a power of 0.5 MW) gives $n_e/n_{e0} \sim \exp(-24)$. Obviously, the theory breaks down at such high power levels; the exponent is of order unity at $P_{\mathrm{rf}} \sim 20$ kW. The reason that the ponderomotive force is much more significant in the ICRF than at lower hybrid frequencies ($f \sim 1$ GHz) is the very strong frequency dependence: $n_e/n_{e0} \propto \exp(-1/\omega^2)$. This phenomenon is therefore intrinsic to the IBW heating scheme in low field devices, since the IBW cannot be launched from the edge of the plasma without a strong parallel electric field in the scrapeoff layer.

Though no direct density measurements adjacent to the antenna were available, indirect evidence of a strong ponderomotive effect was obtained from analysis of the *reactive* component of the antenna loading. The reactive loading is defined as the change in inductive reactance from the vacuum value, assuming a fixed antenna capacitance. The inductance decreases from its vacuum valve as the separation between the plasma and the antenna strap decreases, therefore the inductance is a measure of the gap between the plasma and the antenna. At a fixed small antenna/plasma gap, the inductance rose towards the vacuum value as the net power was raised, indicating a substantial local density depletion. In Fig. 5, the reactive loading as a function of net rf power is shown for an inside-wall-limited discharge with a gap of 0.3 cm between the last closed flux surface and the outside limiter. In this case, the 32 MHz rf power was ramped slowly from 0 to 0.45 MW. Also shown are measurements of the reactive loading from a series of similar discharges where the outer gap was varied by changing the vertical field. The density depletion evidently saturated at about 0.25 MW, yielding a density near the antenna similar to that obtained at 35 kW with an outer gap of 7 cm. For plasmas with lower edge densities (obtained with larger outer gaps, or in diverted discharges), the effect saturated at lower power levels. For diverted discharges with an outer gap greater than a few centimeters, the saturated power level was at or below the minimum measurable power (about 0.5 kW).

Most of the observed features of the IBW loading can be reasonably explained by a linear loading model wherein the effect of the ponderomotive force is taken into account in a somewhat *ad hoc* manner.[9] In this simplified, not fully self-consistent model, the density is assumed to be zero at the face of the Faraday shield, and to rise linearly to join with the density measured at the limiter radius. In particular, the model accounts in a semi-quantitative way for the observed phase dependence of the loading, when the phase difference between the two straps was varied from 0° to 180°.

The success of this model in accounting for the observed IBW antenna loading indicates that a reasonable understanding of this aspect of the experimental results has been reached. However, this does not explain the apparent lack of penetration of the rf power to the center of the discharge: in the linear picture, the EPW propagating along resonance cones in the edge of the plasma should mode-transform to the IBW at $\omega = \omega_{LH}$. However, several effects complicate the situation. Even in the linear regime, ion Bernstein waves that are excited by the EPW fields at locations significantly above or below the midplane tend to be strongly electron Landau damped in the edge region.[10,11] In addition, the ponderomotive force will tend to locally depress the density along the resonance cone trajectories, preventing the EPW from reaching the mode transformation layer as long as the electric field intensity is large. The nonlinearly propagating EPW would therefore be trapped in the edge region until the wave energy is dissipated by electron transit time effects or parametric decay instabilities (PDI).

Since the parametric instability driving force is proportional to $\sim (v_{D\parallel}/v_{ph\parallel})^2$ and $\sim (v_{D\perp}/v_{ph\perp})^2$, where $v_{D\perp} = cE_{0\perp}/B_0$ is the $\vec{E}_{0\perp} \times \vec{B}_0$ rf drift velocity and $v_{phj} = \omega/k_j$ is the appropriate component of the wave phase velocity, the strong electric fields that result from the low group velocity of the EPW near the mode transformation point and of the IBW can drive PDI in addition to the ponderomotive effect. Indeed, as was first reported in Ref. 1, parametric decay of the pump wave into two lower frequency waves was often observed during IBW injection in DIII–D. In many cases, the decay waves were identified as an ion cyclotron quasimode (ICQ) and a IBW at a frequency lower than the pump. The frequency of the ICQ was equal to the fundamental ion cyclotron frequency of either deuterium or hydrogen at a major radius nearly equal to that of the IBW antenna, implying that the location of the decay was near the low-field side of the plasma, *i.e.*, near the antenna.

The PDI observed in the DIII–D IBW experiments have been studied in some detail.[12] Only a brief summary of these results will be given here. Under conditions where the line-averaged plasma density is relatively low ($\bar{n}_e \lesssim 2 \times 10^{13}\,\mathrm{cm}^{-3}$) and the scrape-off layer density relatively high ($n_{SOL} \gtrsim 1 \times 10^{11}\,\mathrm{cm}^{-3}$), such as obtained in inside-wall limited discharges, a remarkably clear correlation between parametric decay activity and edge ion heating was observed. A typical parametric decay spectrum is shown in Fig. 6, along with the hydrogen neutral-particle charge-exchange spectrum observed during the same discharge. Both hydrogen and deuterium ions showed high-energy perpendicular tail formation; no parallel heating was observed. The time behavior of the charge exchange signal indicated that the confinement time of the high-energy ions is $\ll 1$ msec. The fact that no ion heating in the bulk plasma was observed, combined with the characteristics of the tail signal, shows that the heating was an edge phenomenon.

The edge deuterium and/or hydrogen heating was clearly correlated with the amplitude of the corresponding ICQ. Both the deuterium heating and the deuterium ICQ amplitude peaked near the toroidal field at which efficient coupling to the IBW is predicted; tail formation and PDI both exhibited a power threshold of several hundred kilowatts; and both the deuterium ICQ amplitude and the deuterium heating were very sensitive to the H/D ratio. It is important to note that the IBW antenna loading showed none of the sensitive dependences exhibited by the PDI amplitudes and by the associated edge ion heating, implying that the wave energy dissipation did not occur in the antenna near field.

Under some conditions, strong electron heating of the plasma in the scrapeoff layer was observed with the Langmuir probe located 2 m away from the IBW antenna. The electron heating could result from parametric decay of the pump fields into a low frequency electron Landau damped (ELD) quasimode or perhaps from electron transit time effects (the strongly nonlinear limit of electron Landau damping) in the spatially localized pump wave field. In some situations, a pump spectrum asymmetrically broadened towards the low frequency side was observed, corresponding to decay into a low frequency ELD quasimode.

In cases where edge heating was well correlated with PDI, estimates of the fraction of the applied rf power required to account for the observed edge ion and electron heating show that the parametric decay can represent an important power sink. More quantitative estimates are difficult due to the substantial uncertainties in the measurements. However, it is clear from these results that the observed PDI constitute a significant dissipation mechanism in the plasma edge region in these experiments, which is not surprising when the strong nonlinearity of this regime is taken into account.

REFERENCES

1 R.I. Pinsker, M.J. Mayberry, M. Porkolab, and R. Prater, *Radio-Frequency Power in Plasmas: Eighth Topical Conference*, Irvine, CA 1989 (American Insitute of Physics, New York, 1989), p. 314.

2 R.H. Goulding, these proceedings.

3 C.C. Petty, R.I. Pinsker, M.J. Mayberry, *et al.*, "Fundamental and Second Harmonic Fast-Wave Heating on DIII–D," these proceedings.

4 C.C. Petty, R.I. Pinsker, M.J. Mayberry, *et al.*, "Direct Electron Heating by 60 MHz Fast Waves on DIII–D," these proceedings.

5 M. Brambilla, Nucl. Fusion **28** (1988) 549.

6 M. Ono, K.L. Wong, and G.A. Wurden, Phys. Fluids **26** (1983) 298.

7 S.C. Chiu, M.J. Mayberry and W.D. Bard, Nucl. Fusion **30** (1990) 2551.

8 M. Porkolab and M. Goldman, Phys. Fluids **19** (1976) 872.

9 S.C. Chiu, *et al.*, these proceedings.

10 M. Ono, G.J. Greene, and S. Bernabei, *Radio-Frequency Power in Plasmas: Eighth Topical Conference*, Irvine, CA 1989 (American Institute of Physics, New York, 1989), p. 306.

11 A. Cardinali and F. Romanelli, *Controlled Fusion and Plasma Physics* (Proc. 18th Conf., Berlin, 1991), **15C**, III, European Physical Society (1991) 273.

12 R.I. Pinsker, C.C. Petty, *et al.*, "Observation of Parametric Decay and Correlated Edge Heating with an Ion Bernstein Wave Antenna on DIII–D," to be published.

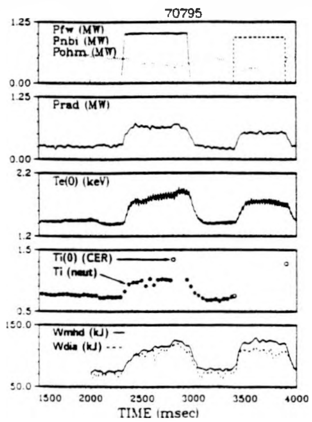

Fig. 1. Time history of fast wave ICH in the D(H) regime and NBI at equal injected power (I_p = 0.7 MA, $\bar{n} = 2 \times 10^{13}$ cm^{-3}).

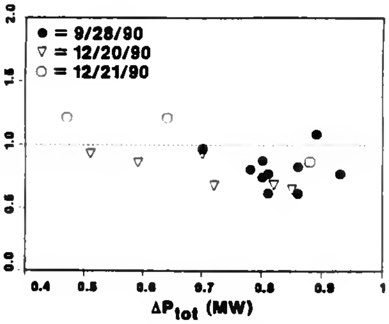

Fig. 2. Absorption efficiency of fast wave ICH in the D(H) regime calculated using ITER–89 linear offset scaling.

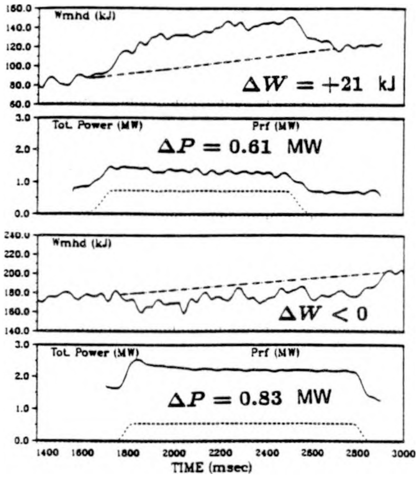

Fig. 3. Time history of stored energy and input power for (a) $2\Omega_H$ FW heating, and (b) $3/2\Omega_H$ IBW heating.

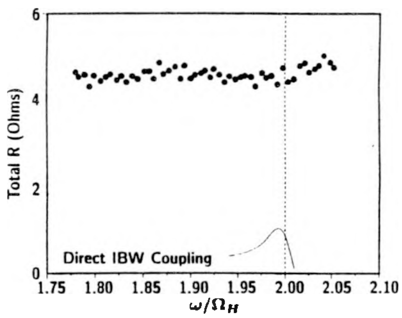

Fig. 4. Experimental (discrete points) and theoretical IBW antenna loading ($I_p = 0.95$ MA, $\bar{n} = 2 \times 10^{13}$ cm^{-3}).

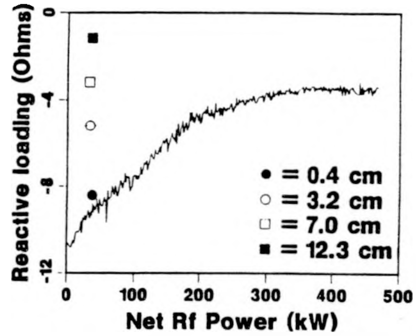

Fig. 5. Reactive component of IBW antenna loading.

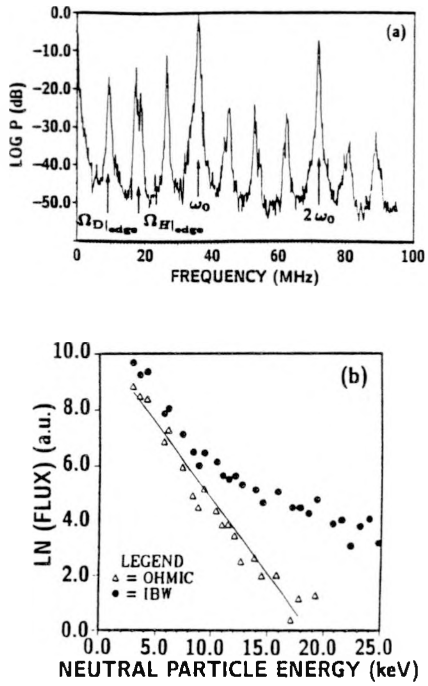

Fig. 6. (a) Parametric decay spectrum observed during 0.8 MW IBW injection. The peak at the 36 MHz generator frequency is saturated to facilitate display of the decay wave peaks. (b) Charge exchange H spectrum showing perpendicular tail formation during IBW ($I_p = 0.9$ MA, $\bar{n} = 2 \times 10^{13}$ cm^{-3}).

GENERAL ATOMICS
P. O. Box 85608 • San Diego, CA • 92186-9784 (619) 455-3000